Metabolism 141 (2023) 155382

Contents lists available at ScienceDirect

Metabolism

journal homepage: www.journals.elsevier.com/metabolism

Evaluation of renal glucose uptake with [^{18}F]FDG-PET: Methodological advancements and metabolic outcomes

Eleni Rebelos [a,b,*], Andrea Mari [c], Vesa Oikonen [a], Hidehiro Iida [a], Pirjo Nuutila [a,d], Ele Ferrannini [b]

[a] Turku PET Centre, University of Turku, Turku, Finland
[b] CNR Institute of Clinical Physiology, Pisa, Italy
[c] CNR Institute of Neuroscience, Padova, Italy
[d] Department of Endocrinology, Turku University Hospital, Turku, Finland

ARTICLE INFO

Keywords:
Positron emission tomography
Kidney
Metabolism
Obesity
Sodium-glucose cotransporter

ABSTRACT

Background/purpose: Studying renal glucose metabolism non-invasively in humans is an unmet need. Positron emission tomography (PET) is the current gold standard for measuring regional tissue glucose uptake rates, but the most widely used glucose analog ([^{18}F]FDG) is not a good substrate for sodium-glucose cotransporters (SGLTs). As a consequence, [^{18}F]FDG spills over into the urine and [^{18}F]FDG-PET considerably underestimates published rates of whole renal glucose uptake obtained using the arterial-venous difference technique. Our aim was to assess whether [^{18}F]FDG-PET can be used in the study of renal glucose metabolism in humans.

Methods: We measured individual [^{18}F]FDG radioactivity in the urine and estimated intraluminal [^{18}F]FDG radioactivity concentration; these values were used to correct renal [^{18}F]FDG-PET data acquired ~90 min from tracer injection under fasting conditions and during an insulin clamp in 9 lean and 16 obese subjects.

Results: We found that the corrected glucose uptake is consistently higher in the medulla than cortex and that both cortical and medullary glucose uptake are higher in lean than obese participants under both fasting and insulinized conditions. Moreover, cortical but not medullary glucose uptake is increased from the fasting to the insulinized condition.

Conclusion: The data show for the first time that [^{18}F]FDG-PET can still provide relevant physiological information on regional renal glucose uptake on the condition that [^{18}F]FDG uptake is corrected for tubular radioactivity.

1. Introduction

The kidney is metabolically very active and demands large amounts of energy for its functions, a large portion being used for the active reabsorption of glucose, sodium, and other solutes from the proximal convoluted tubule (PCT) [1,2]. Along with the marked differences in perfusion and function, several metabolic differences have been described between the renal cortex and medulla. Tubular cells in the cortex are rich in mitochondria and depend predominantly on oxidative metabolism, with fatty acids, ketone bodies, and lactate being the preferred substrates [3]. Insulin receptors are abundantly expressed in the cortex, a region that also contributes to gluconeogenesis thanks to the exclusive expression of key gluconeogenic enzymes (glucose-6-phosphatase, fructose-1,6-biphosphatase, and phosphoenolpyruvate carboxykinase) [4,5]. On the other hand, cells in the inner medulla have fewer mitochondria and depend predominantly on glycolysis for energy production [6,7]; here, glycogen is present at higher concentrations than in the cortex.

The study of renal substrate handling *in vivo* requires catheterization of the renal vein (RV) and an artery (A) (for the determination of substrate A-RV differences) and measurement of renal blood flow. These measures usually show high within-subject variability even under stable metabolic conditions as small A-RV differences are multiplied by a large blood flow (~1.2 L/min). The case of glucose is further complicated by

Abbreviations: AV, arterial-venous; BMI, body mass index; FUR, fractional uptake rate; GLUT, glucose transporters; GU, glucose uptake; PCT, proximal convoluted tubule; PET, positron emission tomography; RGU, renal glucose uptake; SGLT, sodium-glucose cotransporter; T2D, type 2 diabetes.

* Corresponding author at: Turku PET Centre, University of Turku, Turku, Finland; CNR Institute of Clinical Physiology, Pisa, Italy.
E-mail address: eleni.rebelos@utu.fi (E. Rebelos).

https://doi.org/10.1016/j.metabol.2022.155382
Received 11 August 2022; Accepted 16 December 2022
Available online 21 December 2022

the fact that the kidneys simultaneously utilize, secrete, and excrete glucose. In fact, the net transrenal glucose gradient typically oscillates around zero in the fasting state, indicating similar rates of concomitant glucose uptake and production. For this reason, the catheterization technique has been combined with the infusion of a glucose tracer (*e.g.*, ^{3}H-glucose) which is taken up by tissues but is neither endogenously made through gluconeogenesis nor recycled to glucose by label rearrangement [8]. With this experimental setup, the fractional tracer extraction across the kidney multiplied by the arterial 'cold' glucose concentration and renal blood flow yields the absolute value of total renal glucose uptake; separate estimation of cortical and medullary glucose disposal is not possible.

Positron emission tomography (PET), presently the gold standard for the non-invasive measurement of tissue metabolic rates *in vivo*, has been widely used in conjunction with the glucose tracer, ^{18}F-labeled-2-fluoro-2-deoxy-D-glucose ([^{18}F]FDG), in studies of glucose utilization in virtually all organs but one, the kidney. This is largely because [^{18}F]FDG, a glucose analog where fluorine-18 substitutes the hydroxyl at the second position in the glucose molecule (hence the acronyms [^{18}F]FDG and 2-FDG have been used interchangeably) is filtered through the glomerulus but virtually not reabsorbed by the sodium-glucose cotransporters (SGLT1 and SGLT2); its accumulation in collecting tubules and pelvis has been thought to interfere with the tissue activity during [^{18}F]FDG-PET scanning [9]. However, to the best of our knowledge attempts to evaluate whether renal [^{18}F]FDG-PET scanning may still provide clinically relevant information have not been performed systematically.

In this study we aimed to correct rates of [^{18}F]FDG uptake for tracer excretion, to compare such rates with published uptake rates obtained by the catheter-tracer technique, and to assess whether [^{18}F]FDG-based regional renal glucose uptake rates can be reliably measured under fasting and euglycemic hyperinsulinemic conditions in healthy lean subjects and obese individuals.

2. Methods

2.1. Study participants and study design

Abdominal [^{18}F]FDG acquisitions were carried out in the fasting state and during a euglycemic insulin clamp on separate days using the same protocol. The details of these studies have been described previously [10–12]. In brief, morbidly obese subjects were recruited from the SLEEVEPASS study, a larger randomized prospective clinical trial comparing different surgical techniques for the treatment of morbid obesity (ClinicalTrials.gov, NCT00793143). Healthy lean controls were also recruited. The exclusion and inclusion criteria have been previously published [10]. All subjects gave informed consent and were screened before they were included in the study. Renal [^{18}F]FDG acquisitions were available in 25 subjects (16 obese and 9 lean) during a euglycemic insulin clamp and in 21 subjects (14 obese and 7 lean) also during the fasting state. For the insulin clamp study, two catheters were inserted in the antecubital veins, one for the administration of radiolabeled tracers (and of glucose and insulin on the insulin clamp study day) and the other for arterialized blood sampling. To obtain arterialized venous blood samples, the arm used for venous blood sampling was warmed with a heating pillow throughout the clamp study, as previously done [12,13]. The euglycemic hyperinsulinemic clamp (*i.e.* the gold standard method for assessing systemic insulin resistance) was performed as previously described [14]; in brief, a primed-continuous insulin infusion was given at a rate of 40 mU·m^{-2}·min^{-1}, followed by a variable 20 % dextrose infusion, in order to maintain plasma glucose levels steady at 5 mmol/L. At ~100 ± 10 min of the clamp, [^{18}F]FDG was injected over 15 s, and dynamic scanning started. Frequent arterialized blood sampling was done every 5, 30, and 60 min for the determination of plasma glucose and radioactivity, insulin, and free fatty acids, respectively. Immediately after the completion of the PET scanning, subjects were instructed to void their bladders in order to measure the amount (in MBq) of [^{18}F]FDG excreted in the urine. Plasma and urinary radioactivity concentrations were measured using an automatic γ-counter (Wizard 1480; Wallac, Turku, Finland). The study protocol was approved by the Ethics Committee of the Hospital District of Southwestern Finland.

2.2. PET data analysis

The PET studies were conducted both in the fasting condition and during the insulin clamp on separate days <2 weeks apart using the GE advanced PET camera (General Electric Medica Systems, Milwaukee, WI). Radioactivity from the abdominal area was acquired 90–120 min from [^{18}F]FDG injection for 15 min (3 × 300 s frames). PET images were reconstructed in a 256 × 256 matrix after correction for decay time, dead time, and photon attenuation. Image analysis was performed using Carimas v.2.9 (http://www.turkupetcentre.fi/). To obtain the time-radioactivity curves, the regions of interest (ROI) were manually drawn on PET/CT fusion images in renal cortex and medulla (Fig. 1). In particular, 4–5 consecutive thin ROIs were drawn using the coronal axis images in the region of slightly lower radioactivity just outside the high signal originating from the renal pyramids; this region of interest was considered to represent the renal cortex [15]. A second thin ROI was drawn more centrally on the same slices, representing the medulla [15]. Data were analysed using the fractional uptake rate (FUR, 1/min). To obtain glucose uptake rates, FUR values were multiplied by the concomitant plasma glucose values. The lumped constant correction that is applied to account for the difference between glucose and [^{18}F]FDG uptake from the studied tissue is not known for the kidneys and was assumed to be 1[16]. Glucose uptake (GU) rates are expressed as μmol·min^{-1}·100 mL^{-1}. Skeletal muscle GU (psoas muscle) was also calculated as FUR, multiplied by plasma glucose levels and divided by the lumped constant for skeletal muscle (1.2) [17].

2.3. Calculations

Estimated glomerular filtration rate (eGFR) was calculated by the Chronic Kidney Disease Epidemiology Collaboration (CKD-EPI) eq. [18]; total eGFR (mL/min) was calculated adjusting for individual body surface area (by the Du Bois&Du Bois formula [19]). FUR and renal GU (RGU) were calculated as described previously [15,20], tubular volume was assumed to be 5 % of the ROI volume [21]. Using the individual PET acquisitions and urine radioactivity values, parameters of renal radioactivity were calculated as detailed in Table 1; in particular, corrected regional [^{18}F]FDG uptake rates were obtained by subtracting late tubular [^{18}F]FDG radioactivity from the ROI activity.

2.4. Calculation of insulin-stimulated glucose disposal (M value)

The M value was calculated as a measure of whole-body insulin sensitivity, as previously described [22], and expressed per kilogram of fat-free mass (μmol·kgFFM^{-1}·min^{-1}), because this normalization minimizes differences due to sex, age, and body weight [23].

2.5. Statistical analysis

Data are summarized as mean ± SD or median and interquartile range (IQR) for variables with non-normal distribution by Wilks-Shapiro test. Group comparisons were carried out using Mann-Whitney *U* test for unpaired observations. Paired comparisons by group were performed by repeated-measure ANOVA. A $p < 0.05$ was considered significant. Analyses were done using JMP version 13.0 (SAS Institute, Cary, NC, USA). Images were created using ggplot package on *R* Studio [24].

3. Results

The lean and obese study groups were well-balanced for sex and age (Table 2). The study groups consisted predominantly of women with

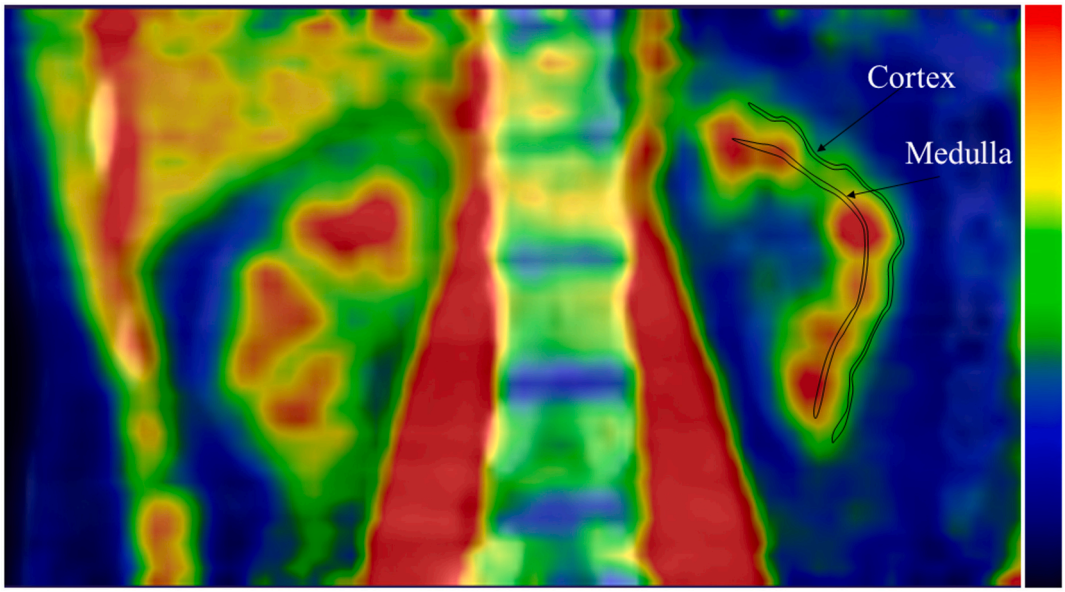

Fig. 1. Example of ROI placement in the renal cortex and medulla.

Table 1
Definition of parameters extracted from [^{18}F]FDG-PET acquisitions.

Parameter	Description	Calculation	Units
PET period	PET period, from [^{18}F]FDG injection to urine collection	PET period, from [^{18}F]FDG injection to urine collection	min
Urine period	Period of urine collection, from pre-study urination to post-PET voiding	Period of urine collection	min
Urine mass	Urine mass	Urine mass	g
Urine flow	Mean urine flow	(Urine mass) / (urine period) (assumes urine density = 1 g/mL)	mL/min
Urine activity	Total urine activity	Urine [^{18}F]FDG activity	MBq
Tubular flow	Estimated mean tubular [^{18}F]FDG flow	(Urine activity) / (PET period)	kBq/min
Mean tubular activity	Estimated mean tubular [^{18}F]FDG activity	(Tubular flow) / (urine flow)	kBq/mL
Late tubular activity	Estimated late tubular [^{18}F]FDG activity	(Urinary clearance) * (mean plasma activity during the late phase) / (urine flow)	kBq/mL
Urinary clearance	Estimated urinary [^{18}F]FDG clearance	(Urine activity) / (integral of the plasma activity curve during the PET period)	mL/min
Renal tissue clearance	Estimated total renal tissue [^{18}F]FDG clearance	(Mean cortex FUR) * (cortex volume) + (mean medulla FUR) * (medulla volume). Cortex and medulla volumes are assumed to be 210 and 75 mL, respectively (both kidneys)	mL/min

Table 2
Clinical and metabolic characteristics of the study subjects.

	Lean	Obese	*p*
M/W	1/8	2/14	ns
Age (years)	48 ± 6	47 ± 9	ns
Body weight (kg)	67 [13]	118 [18]	<0.0001
BMI (kg/m^2)	23.3 [3.5]	43.2 [4.5]	<0.0001
M value (μmol·min^{-1}·kg^{-1})	41.7 [19.3]	8.4 [2.8]	<0.0001
eGFR (mL/min)	96 ± 12	132 ± 17	0.0007
Plasma glucose (mmol/L)	5.4 ± 0.3	6.0 ± 0.9	ns
Plasma insulin (pmol/L)	30 [6]	90 [70]	0.004
Fasting muscle FUR (1/min)	0.002 [0.001]	0.002 [0.001]	ns
Fasting muscle GU (μmol·min^{-1}·100 mL^{-1})	1.04 [0.30]	0.97 [0.29]	ns
Clamp muscle FUR (1/min)	0.013 [0.015]	0.004 [0.008]	0.004
Clamp muscle GU (μmol·min^{-1}·100 mL^{-1})	5.42 [5.77]	1.59 [2.97]	0.006

Entries are mean ± SD or median [interquartile range]; *p* value for the comparison obese *vs* lean subjects.

data of three men (one lean and two obese) available in the fasting and insulin clamp experiments. As expected, obese subjects had markedly impaired whole-body insulin sensitivity, as indicated by the M value. Skeletal muscle GU was similar in the fasting state, and markedly reduced on the clamp, in the obese *vs* lean. Total eGFR (mL/min) was higher in the obese subjects.

3.1. Urinary [^{18}F]FDG excretion and tubular concentration (Table 3)

In the fasting state, total urine decay-corrected [^{18}F]FDG radioactivity averaged 18 % of the injected dose over ~120 min, similarly in lean and obese subjects. Urinary [^{18}F]FDG clearance averaged ~35 % of eGFR in lean individuals and ~40 % in the obese. Mean tubular [^{18}F]FDG flow averaged ~240 kBq/min, resulting in estimated mean and late tubular [^{18}F]FDG activity of 70 and 45 kBq/mL, without differences between lean and obese. Renal tissue [^{18}F]FDG clearance was 10–15 times smaller than urinary [^{18}F]FDG clearance, and was significantly impaired in the obese compared to the lean group. On the clamp day, a smaller fraction of the injected [^{18}F]FDG dose was recovered in the urine than on the fasting day, and more so in the lean. In contrast, urinary [^{18}F]FDG clearance was similar between fasting and insulin in either group. Tubular [^{18}F]FDG flow was smaller with insulin compared to fasting, as were measures of [^{18}F]FDG tubular activity. These differences can be attributed to a greater sequestration of the [^{18}F]FDG dose in insulin-stimulated tissues such as skeletal muscle, and the consequent reduction of average plasma [^{18}F]FDG activity. In line with this, tubular flow, mean and tubular late activity were all inversely related to the M value (Supplemental Fig. 1). Of note, insulin-stimulated renal tissue [^{18}F]FDG clearance, while still lower in the obese, was only slightly – and statistically non-significantly – higher than under fasting conditions.

Table 3
[^{18}F]FDG radioactivity parameters in lean and obese subjects[a].

	Lean	Obese	p*
Fasting			
Urine radioactivity (MBq), % of dose	32 [19], 17 %	36 [13], 19 %	ns
[^{18}F]FDG dose (MBq)	190 [16]	189 [11]	ns
Urine volume (mL)	350 [400]	500 [335]	ns
Urinary [^{18}F]FDG clearance (mL/min)	35 [20]	54 [26]	0.04
Mean urinary flow (mL/min)	2.6 [2.9]	3.7 [3.8]	ns
Tubular [^{18}F]FDG flow (kBq/min)	217 [107]	269 [100]	ns
Mean tubular [^{18}F]FDG activity (kBq/mL)	76 [58]	65 [37]	ns
Late tubular [^{18}F]FDG activity (kBq/mL)	46 [50]	45 [48]	ns
Renal tissue [^{18}F]FDG clearance (mL/min)	2.5 [0.7]	1.7 [0.5]	0.001
Insulin clamp			
Urine radioactivity (MBq), % of dose	15 [8], 8 %	23 [16], 12 %#	0.03
[^{18}F]FDG dose (MBq)	184 [14]	186 [10]	ns
Urine volume (mL)	700 [293]	580 [440]	ns
Urinary [^{18}F]FDG clearance (mL/min)	49 [31]	52 [25]	ns
Mean urinary flow (mL/min)	4.6 [1.8]	3.6 [3.5]	ns
Tubular [^{18}F]FDG flow (kBq/min)	103 [45]#	126 [99]#	ns
Mean tubular [^{18}F]FDG activity (kBq/mL)	22 [22]#	37 [36]#	0.04
Late tubular [^{18}F]FDG activity (kBq/mL)	3.4 [3.2]#	13.2 [25.7]#	0.002
Renal tissue [^{18}F]FDG clearance (mL/min)	2.7 [0.9]	1.9 [0.7]	0.007

Entries are median [interquartile range].
* p value for the difference between obese and lean individuals.
# $p < 0.05$ or less for the comparison between fasting and insulin in each group.
[a] Complete urinary data were available in 20 subjects during insulin clamp and 13 subjects during fasting conditions.

3.2. Regional [^{18}F]FDG uptake (Table 4)

In the fasting state, both cortical and medullary [^{18}F]FDG FUR and uptake rates – whether using corrected or uncorrected values – were higher in lean than obese subjects. The pattern of differences was similar in the clamp experiments (Fig. 2A). These results held true also when accounting for eGFR for all regions ($p < 0.05$), except for fasting medullary GU which only trended to be higher in healthy controls compared to patients with obesity ($p = 0.07$). Insulin appeared to have no stimulatory effect on either cortical or medullary [^{18}F]FDG FUR and uptake rates when using uncorrected values. However, when these rates were corrected for the individual tubular [^{18}F]FDG radioactivity value, the effect of insulin became clear, and statistically significant, for cortical but not medullary ROIs in both groups without canceling the difference in the GU rates between the two groups (73 % increase in the lean participants).

In the pooled data, [^{18}F]FDG uptake was well correlated with skeletal muscle [^{18}F]FDG uptake in the cortex but not the medulla (Fig. 2B–C).

4. Discussion

The general conclusion of the present study is that the [^{18}F]FDG-PET technique can be used to study regional renal glucose uptake on the condition that urine is carefully collected and its [^{18}F]FDG radioactivity measured, and that these measurements are used to correct tissue [^{18}F]FDG uptake for tubular radioactivity. In particular, late acquisition of renal radioactivity (~90 min following [^{18}F]FDG injection in the present study) is mandatory in order to minimize radioactivity inside the tubuli. Then, the only parameter necessary for the method is total tubular volume, which had to be assumed as we know of no way to measure

Table 4
Regional [^{18}F]FDG uptake.

	Lean	Obese	p
Fasting			
Cortical FUR (1/min)	0.008 [0.002] [0.002]	0.005 [0.002]	0.002
Cortical GU (μmol·min^{-1}·100 mL^{-1})	4.1 [1.7]	2.7 [1.3]	0.005
Corr. cortical GU (μmol·min^{-1}·100 mL^{-1})	2.2 [1.6]	−0.1 [3.8]	0.008
Medullary FUR (1/min)	0.013 [0.004]	0.009 [0.002]	0.003
Medullary GU (μmol·min^{-1}·100 mL^{-1}) (μmol/100 g/min)	7.5 [2.4]	5.1 [1.5]	0.01
Corr. medullary GU (μmol·min^{-1}·100 mL^{-1})	6.6 [6.9]§	2.4 [3.2]§	0.008
Insulin clamp			
Cortical FUR (1/min)	0.008 [0.003]	0.006 [0.002]	0.003
Cortical GU (μmol·min^{-1}·100 mL^{-1})	4.2 [1.0]	2.7 [1.0]	0.004
Corr. cortical GU (μmol·min^{-1}·100 mL^{-1})	3.8 [0.9]#	1.2 [1.6]#	0.0008
Medullary FUR (1/min)	0.011 [0.005]	0.009 [0.003]	0.046
Medullary GU (μmol·min^{-1}·100 mL^{-1})	5.4 [2.7]	4.1 [1.1]	0.04
Corr. medullary GU (μmol·min^{-1}·100 mL^{-1})	5.0 [2.9]§	2.9 [1.3]§	0.002

Entries are median [interquartile range]; FUR = fractional uptake rate; GU = glucose uptake; Corr. GU = value corrected for tubular radioactivity; p value for the group comparison obese *vs* lean subjects. Complete urinary data were available in 20 subjects during insulin clamp and 13 subjects during fasting conditions.
# $p < 0.05$ or less for the paired comparison of insulin *vs* fasting in both groups (repeated measures ANOVA).
§ $p < 0.05$ or less for the paired comparison of medullary *vs* cortical in both groups (repeated measures ANOVA).

tubular volume *in vivo* directly. The fraction we used, 5 % of ROI volume, has been determined by anatomical studies [21]. In our analysis, this value is used as a constant across subjects (lean or obese) and physiological condition (fasting or euglycemic hyperinsulinemia).

The data used for this study yielded several outcomes. With regard to the urinary parameters, urinary [^{18}F]FDG clearance – averaging 35 mL/min or 1/3 of eGFR in our lean subjects – is in the same range (31 mL/min) as that measured for glucose in a group of healthy individuals in whom SGLT reabsorptive capacity had been saturated by clamping plasma glucose at 22 mmol/L [25]. This finding can be taken as direct evidence that in humans 2-FDG has minimal affinity for SGLTs, as previously demonstrated in mice transfected with human SGLTs and GLUT2 [26]. Therefore, 2-FDG uptake into renal tissues must occur from the peritubular circulation through the GLUT2 transporter that is expressed on the basolateral membrane of the proximal convoluted tubule, for which 2-FDG has even higher affinity than D-glucose [26]. Of note, transport of D-glucose from the luminal side to the circulation *via* GLUT2 is down the concentration gradient created by SGLT-mediated glucose absorption, while transport of 2-FDG *via* GLUT2 is down an inverse gradient given by the minimal 2-FDG concentration in the cell.

Given the differential transport route of D-glucose and 2-FDG, it is expected that values for renal glucose uptake obtained by the catheter/tracer glucose technique should be different from those calculated by [^{18}F]FDG-PET. To gauge this difference, we compiled the published human studies that have used the catheter/tracer technique (Table 5). The values for total renal glucose uptake in 6 studies in healthy controls in the fasting state show substantial interstudy variability. The corresponding [^{18}F]FDG-PET estimate (obtained by multiplying the renal tissue clearance in Table 3 by the mean fasting glycemia) is 14 μmol/min, which seems to be a considerable underestimate of the catheter data. Importantly, for skeletal muscle the two techniques (Tables 5 and 1) measure very close values in the fasting state (0.84 *vs* 1.04

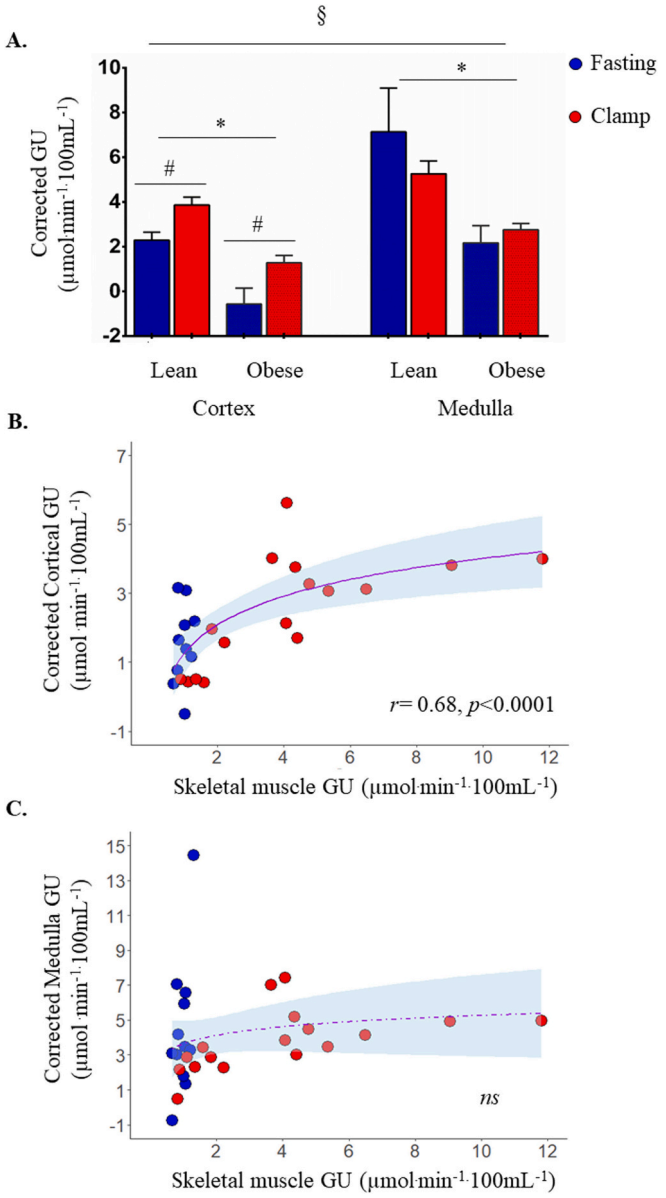

Fig. 2. Bar graph showing corrected cortical and medullary glucose uptake rates in the two groups under two metabolic conditions. Data are mean ± SEM. $^{*}p < 0.05$ in the comparison between obese and lean participants, $^{\#}p < 0.05$ for the comparison between fasting and insulin clamp and $^{\S}p < 0.05$ for the comparison between cortex and medulla (A). In the pooled fasting (blue circles) and insulin clamp (red circles) data, corrected cortical (B) but not medullary GU (C) correlates with skeletal muscle glucose uptake.

µmol·min^{-1}·100 mL^{-1}) as well during similar euglycemic hyperinsulinemia (6.5 *vs* 5.4 µmol·min^{-1}·100 mL^{-1}); the same has been previously reported for myocardial muscle [27]. Clearly, the physiological differences between muscle (GLUT4-mediated uptake of blood-borne glucose) and kidney (GLUT2-mediated 2-FDG uptake from the peritubular capillary network) account for the discrepant quantitative performance of 2-FDG in the two tissues. Another mechanism leading to an underestimation of renal glucose uptake by [^{18}F]FDG might be dephosphorylation of "trapped" [^{18}F]FDG, given that the kidneys express the enzyme glucose-6-phosphatase. However, this process cannot be identified – let alone quantified – *in vivo*, and therefore remains a theoretical issue.

Unlike the catheter method, however, [^{18}F]FDG-PET can provide quantitative estimates of regional glucose uptake rates in the kidney. Using the corrected uptake rates (Table 4), our analysis yields relevant physiological findings. Firstly, in medullary ROIs [^{18}F]FDG uptake was higher than in cortical ROIs, in agreement with *in vitro* results [6,7], showing that the medulla is a preferential user of glucose as an energy substrate while in the cortex free fatty acid use and gluconeogenesis predominate [3]. Secondly, physiological hyperinsulinemia stimulated cortical but not medullary [^{18}F]FDG uptake, in line with evidence that renal ATP is higher in the cortex than in the medulla [28] and insulin receptors are expressed on the basolateral side of tubular cells [29]. Importantly, the 73 % increment of cortical [^{18}F]FDG uptake with insulin is of similar magnitude as the 84 % increase estimated by the catheter/tracer technique for total renal glucose uptake [30] (Table 5). Thirdly, [^{18}F]FDG uptake was markedly reduced in the obese group in both cortex and medulla (Table 4). To a first approximation, this finding is in agreement with the fact that the expression of insulin receptors and the levels of tyrosine phosphorylated receptors are reduced in the renal cortex of insulin resistant rat models [31] and in the proximal convoluted tubular cells of both human and rat diabetic kidney [32]. However, insulinization did not significantly stimulate medullary [^{18}F]FDG uptake (Fig. 2), yet medullary [^{18}F]FDG uptake was significantly reduced in the obese both during fasting and following insulin. Obesity is a risk factor for chronic kidney disease [33,34]. In the obese, the higher metabolic demand leads to a maladaptive increase in single-nephron GFR, eventually resulting in nephron loss [35].

To the best of our knowledge, this study is the first systematic attempt to assess whether [^{18}F]FDG-PET can yield useful clinical information regarding renal glucose metabolism. However, several limitations must be acknowledged. First, the volumes of fluid (saline and intravenous glucose infusions) given during the studies, and the salt intake of the subjects were not recorded; aggressive hydration has been shown to enhance [^{18}F]FDG elimination in the urine [36], whereas salt intake may affect the renal insulin receptor density [37]. Second, even though it has been described that patients with obesity and proteinuria have epithelial hypertrophy and increased tubular urinary spaces compared to lean subjects [38], we applied a 5 % correction for the intraluminal tubular volume for both groups, since there are no other published estimates of this quantity in patients with obesity. At any rate, a fixed correction would underestimate rather than overestimate the reported differences in renal glucose uptake values between patients with obesity and lean controls. Also, a more rigorous modelling approach for the estimation of the renal [^{18}F]FDG dynamics would have required simultaneous acquisitions of aorta, kidney and bladder; this was not possible in the present study, but may be possible with the use of the new state-of-the-art PET scanners (FOV ~1.1 m). These limitations could help planning future studies investigating renal glucose metabolism *in vivo*, in addition to suggesting the use of glucose analogs, such as 6-fluoro-6-deoxy-D-glucose, that are transported through SGLTs and could therefore closely trace renal glucose transport [39]. It must also be acknowledged that not only is the catheter/tracer technique invasive, but that it is fraught with high variability as null tracer exchange across the kidney has been reported [40]. Indeed, in a very recent study, Tripathy et al. measured renal glucose uptake rates in fasting conditions and following treatment with SGLT2-i [41]. Under fasting conditions, their renal glucose uptake rates were substantially smaller than what has been previously reported in the literature and in closer agreement to our PET measurements (Table 5). Finally, because of the close proximity of the cortical and medullary ROIs some interference between the cortical and medullary results cannot be excluded – even though this would affect the current results minimally.

In conclusion, albeit 2-FDG does not fully trace native glucose, our 'advanced' renal [^{18}F]FDG-PET methodology here applied on patients with obesity and healthy lean controls provides strong support for the notion that the human renal cortex is an insulin sensitive tissue; additional metabolic information can be at hand.

Supplementary data to this article can be found online at https://doi.org/10.1016/j.metabol.2022.155382.

Table 5
Renal and skeletal muscle rates of glucose uptake as measured by the AV difference/tracer technique.[a]

Reference	Organ	Condition	Subjects	Glucose uptake (μmol·min^{-1})	Glucose uptake# (μmol·min^{-1}·100 g)	Conversion/notes
AV difference						
Nieth et al. [42]	Kidney	–	71 KD	Negligible	Negligible	–
Wahren et al. [43]	Kidney	Fasting	5 T1D	323	108	Not corrected for glycosuria
Stumvoll et al. [44]	Kidney	Fasting	10 HC	181	60	Body weight: 80 kg
Meyer et al. [45]	Kidney	Fasting	12 HC	93	31	Body weight: 72 kg
Meyer et al. [46]	Kidney	Fasting	14 T2D	353	118	BMI: 28.1 kg/m^2, assumed height 1.7 m
Meyer et al. [46]	Kidney	Fasting	15 HC	103	34	BMI: 27.8 kg/m^2, assumed height 1.7 m
Cersosimo et al. [30]	Kidney	Fasting	18 HC	117	39	Body weight: 71 kg
Cersosimo et al. [30]	Kidney	Insulin	6 HC	203	68	Insulin infusion rate: 0.125 mU·kg^{-1}·min^{-1}
Cersosimo et al. [30]	Kidney	Insulin	8 HC	235	78	Insulin infusion rate: 0.25 mU·kg^{-1}·min^{-1}
Meyer et al. [47]	Kidney	Fasting	10 T2D	375	125	Body weight: 85.1 kg
Meyer et al. [47]	Kidney	OGTT	10 T2D	427	142	Corrected for glycosuria
Meyer et al. [47]	Kidney	Fasting	10 HC	84	28	Body weight: 92.8 kg
Meyer et al. [47]	Kidney	OGTT	10 HC	202	67	Body weight: 92.8 kg
Tripathy et al. [41]	Kidney	Fasting	9 HC	38.3	0.044	BMI: 30.1 kg/m^2, assumed height 1.7 m
Tripathy et al. [41]	Kidney	Fasting	13 T2D	32.2	0.037	BMI: 30.1 kg/m^2, assumed height 1.7 m
Tripathy et al. [41]	Kidney	SGLT2-i	9 HC	130.5	0.15	BMI: 30.1 kg/m^2, assumed height 1.7 m
Tripathy et al. [41]	Kidney	SGLT2-i	13 T2D	168	0.193	BMI: 30.1 kg/m^2, assumed height 1.7 m
Baron et al. [48]	Leg muscle	Fasting	8 HC	151.5	0.44	Estimated leg weight: 10 kg
Baron et al. [49]	Leg muscle	Insulin	8 HC	151.5	0.84	Insulin infusion rate: 15 mU·m^{-2}·min^{-1}
Baron et al. [49]	Leg muscle	Insulin	6 HC	273	13.2	Insulin infusion rate: 300 mU·m^{-2}·min^{-1}
DeFronzo et al. [50]	Leg muscle	Fasting	10 HC	99.9	0.83	Estimated leg weight:12 kg
DeFronzo et al. [50]	Leg muscle	Insulin	10 HC	588.4	6.5	Insulin infusion rate: 40 mU·m^{-2}·min^{-1}
[^{18}F]FDG-PET						
Dadson et al. [20]	Leg muscle	Insulin	14 HC	725	7.25	40 mU·m^{-2}·min^{-1}; 10 kg leg
Dadson et al. [20]	Leg muscle	Insulin	23 obese	220	2.20	40 mU·m^{-2}·min^{-1}; 10 kg leg

[a] HC: healthy controls; T1D and T2D: type 1 and type 2 diabetes; KD: kidney disease.

CRediT authorship contribution statement

ER analysed the data and drafted the manuscript. VO and AM analysed the data. PN acquired the data. EF analysed the data and critically revised the text. All authors approved the final version of the text. PN and EF are the guarantors of this work.

Conflict of interest

None.

Acknowledgments

The authors thank the staff of the Turku PET Centre for performing the PET imaging.

Funding

The study was conducted within the Center of Excellence in Cardiovascular and Metabolic Diseases, supported by the Academy of Finland, the University of Turku, Turku University Hospital, Åbo Akademi University, Finnish Diabetes Foundation, Sigrid Jusélius Foundation. ER reports funding from the Emil Aaltonen Foundation, the Finnish Cultural Foundation, the Paulo Foundation, the Maud Kuistilan Muistosäätiö, the Finnish Diabetes Research Foundation, and from the Finnish Medical Foundation.

Ethical approval

All procedures performed in studies involving human participants were in accordance with the ethical standards of the institutional and/or national research committee and with the 1964 Helsinki declaration and its later amendments or comparable ethical standards.

References

[1] Owen OE, Felig P, Morgan AP, Wahren J, Cahill GFJ. Liver and kidney metabolism during prolonged starvation. J Clin Invest 1969;48:574–83. https://doi.org/10.1172/JCI106016.

[2] Féraille E, Doucet A. Sodium-potassium-adenosinetriphosphatase-dependent sodium transport in the kidney: hormonal control. Physiol Rev 2001;81:345–418. https://doi.org/10.1152/physrev.2001.81.1.345.

[3] Balaban RS, Mandel LJ. Metabolic substrate utilization by rabbit proximal tubule. An NADH fluorescence study. Am J Physiol 1988;254:F407–16. https://doi.org/10.1152/ajprenal.1988.254.3.F407.

[4] Schmid H, Scholz M, Mall A, Schmidt U, Guder WG, Dubach UC. Carbohydrate metabolism in rat kidney: heterogeneous distribution of glycolytic and gluconeogenic key enzymes. Curr Probl Clin Biochem 1977;8:282–9.

[5] Mather A, Pollock C. Glucose handling by the kidney. Kidney Int Suppl 2011:S1–6. https://doi.org/10.1038/ki.2010.509.

[6] Lee JB, Vance VK, Cahill GFJ. Metabolism of C14-labeled substrates by rabbit kidney cortex and medulla. Am J Physiol 1962;203:27–36. https://doi.org/10.1152/ajplegacy.1962.203.1.27.

[7] Meury L, Noël J, Tejedor A, Sénécal J, Gougoux A, Vinay P. Glucose metabolism in dog inner medullary collecting ducts. Ren Physiol Biochem 1994;17:246–66. https://doi.org/10.1159/000173829.

[8] Landau BR, Wahren J. Nonproductive exchanges: the use of isotopes gone astray. Metabolism 1992;41:457–9. https://doi.org/10.1016/0026-0495(92)90199-k.

[9] Szabo Z, Xia J, Mathews WB, Brown PR. Future direction of renal positron emission tomography. Semin Nucl Med 2006;36:36–50. https://doi.org/10.1053/j.semnuclmed.2005.08.003.

[10] Helmiö M, Victorzon M, Ovaska J, Leivonen M, Juuti A, Jaser N, et al. SLEEVEPASS: a randomized prospective multicenter study comparing laparoscopic sleeve gastrectomy and gastric bypass in the treatment of morbid obesity: preliminary results. Surg Endosc 2012;26:2521–6. https://doi.org/10.1007/s00464-012-2225-4.
[11] Immonen H, Hannukainen JC, Iozzo P, Soinio M, Salminen P, Saunavaara V, et al. Effect of bariatric surgery on liver glucose metabolism in morbidly obese diabetic and non-diabetic patients. J Hepatol 2014;60:377–83. https://doi.org/10.1016/j.jhep.2013.09.012.
[12] Rebelos E, Immonen H, Bucci M, Hannukainen JC, Nummenmaa L, Honka M-J, et al. Brain glucose uptake is associated with endogenous glucose production in obese patients before and after bariatric surgery and predicts metabolic outcome at follow-up. Diabetes Obes Metab 2019;21:218–26. https://doi.org/10.1111/dom.13501.
[13] Seghieri M, Rebelos E, Gastaldelli A, Astiarraga BD, Casolaro A, Barsotti E, et al. Direct effect of GLP-1 infusion on endogenous glucose production in humans. Diabetologia 2013;56:156–61. https://doi.org/10.1007/s00125-012-2738-3.
[14] Rebelos E, Honka M-J. PREDIM index: a useful tool for the application of the euglycemic hyperinsulinemic clamp. J Endocrinol Invest 2021;44:631–4. https://doi.org/10.1007/s40618-020-01352-z.
[15] Rebelos E, Dadson P, Oikonen V, Iida H, Hannukainen JC, Iozzo P, et al. Renal hemodynamics and fatty acid uptake: effects of obesity and weight loss. Am J Physiol Endocrinol Metab 2019;317:E871–8. https://doi.org/10.1152/ajpendo.00135.2019.
[16] Lindholm P, Minn H, Leskinen-Kallio S, Bergman J, Ruotsalainen U, Joensuu H. Influence of the blood glucose concentration on FDG uptake in cancer–a PET study. J Nucl Med 1993;34:1–6.
[17] Peltoniemi P, Lönnroth P, Laine H, Oikonen V, Tolvanen T, Grönroos T, et al. Lumped constant for [(18)F]fluorodeoxyglucose in skeletal muscles of obese and nonobese humans. Am J Physiol Endocrinol Metab 2000;279:E1122–30. https://doi.org/10.1152/ajpendo.2000.279.5.E1122.
[18] Levey AS, Stevens LA, Schmid CH, Zhang YL, Castro 3rd AF, Feldman HI, et al. A new equation to estimate glomerular filtration rate. Ann Intern Med 2009;150:604–12. https://doi.org/10.7326/0003-4819-150-9-200905050-00006.
[19] Du Bois D, Du Bois EF. A formula to estimate the approximate surface area if height and weight be known. 1916. Nutrition 1989;5:303.
[20] Dadson P, Landini L, Helmiö M, Hannukainen JC, Immonen H, Honka MJ, et al. Effect of bariatric surgery on adipose tissue glucose metabolism in different depots in patients with or without type 2 diabetes. Diabetes Care 2016;39:292–9. https://doi.org/10.2337/dc15-1447.
[21] Snyder WS, Cook MJ, Nasset ES, Karhausen LR, Howells GPTI. Report of the Task Group on Reference Man. A Report Prepared by a Task Group of Committee 2 of the International Commission on Radiological Protection. Pergamon Press; 1975.
[22] Rebelos E, Bucci M, Karjalainen T, Oikonen V, Bertoldo Alessandra, Hannukainen JC, et al. Insulin resistance is associated with enhanced brain glucose uptake during euglycemic hyperinsulinemia: a large-scale PET cohort. Diabetes Care 2021;44:1–7. https://doi.org/10.2337/dc20-1549.
[23] Gastaldelli A, Casolaro A, Pettiti M, Nannipieri M, Ciociaro D, Frascerra S, et al. Effect of pioglitazone on the metabolic and hormonal response to a mixed meal in type II diabetes. Clin Pharmacol Ther 2007;81:205–12. https://doi.org/10.1038/sj.clpt.6100034.
[24] Wickham H. Elegant graphics for data analysis. Springer-Verlag; 2016.
[25] Ferrannini E, Pereira-Moreira R, Seghieri M, Rebelos E, Souza AL, Chueire VB, et al. Insulin enhances renal glucose excretion: relation to insulin sensitivity and sodium-glucose cotransport. BMJ Open Diabetes Res Care 2020:8. https://doi.org/10.1136/bmjdrc-2020-001178.
[26] Sala-Rabanal M, Hirayama BA, Ghezzi C, Liu J, Huang S-C, Kepe V, et al. Revisiting the physiological roles of SGLTs and GLUTs using positron emission tomography in mice. J Physiol 2016;594:4425–38. https://doi.org/10.1113/JP271904.
[27] Paternostro G, Camici PG, Lammerstma AA, Marinho N, Baliga RR, Kooner JS, et al. Cardiac and skeletal muscle insulin resistance in patients with coronary heart disease. A study with positron emission tomography. J Clin Invest 1996;98:2094–9. https://doi.org/10.1172/JCI119015.
[28] Parivar F, Narasimhan PT, Ross B. Renal corticomedullary metabolite gradients during graded arterial occlusion: a localized 31P magnetic resonance spectroscopy study. J Am Soc Nephrol 1991;2:200–11. https://doi.org/10.1681/ASN.V22200.
[29] Talor Z, Emmanouel DS, Katz AI. Insulin binding and degradation by luminal and basolateral tubular membranes from rabbit kidney. J Clin Invest 1982;69:1136–46. https://doi.org/10.1172/jci110549.
[30] Cersosimo E, Garlick P, Ferretti J. Insulin regulation of renal glucose metabolism in humans. Am J Physiol 1999;276:E78–84. https://doi.org/10.1152/ajpendo.1999.276.1.E78.
[31] Tiwari S, Halagappa VKM, Riazi S, Hu X, Ecelbarger CA. Reduced expression of insulin receptors in the kidneys of insulin-resistant rats. J Am Soc Nephrol 2007;18:2661–71. https://doi.org/10.1681/ASN.2006121410.
[32] Gatica R, Bertinat R, Silva P, Carpio D, Ramírez MJ, Slebe JC, et al. Altered expression and localization of insulin receptor in proximal tubule cells from human and rat diabetic kidney. J Cell Biochem 2013;114:639–49. https://doi.org/10.1002/jcb.24406.
[33] Kramer H, Luke A, Bidani A, Cao G, Cooper R, McGee D. Obesity and prevalent and incident CKD: the hypertension detection and follow-up program. Am J Kidney Dis 2005;46:587–94. https://doi.org/10.1053/j.ajkd.2005.06.007.
[34] Moriconi D, Nannipieri M, Dadson P, Rosada J, Tentolouris N, Rebelos E. The beneficial effects of bariatric-surgery-induced weight loss on renal function. Metabolites 2022:12. https://doi.org/10.3390/metabo12100967.
[35] D'Agati VD, Chagnac A, de Vries APJ, Levi M, Porrini E, Herman-Edelstein M, et al. Obesity-related glomerulopathy: clinical and pathologic characteristics and pathogenesis. Nat Rev Nephrol 2016;12:453–71. https://doi.org/10.1038/nrneph.2016.75.
[36] Moran JK, Lee HB, Blaufox MD. Optimization of urinary FDG excretion during PET imaging. J Nucl Med 1999;40:1352–7.
[37] Catena C, Cavarape A, Novello M, Giacchetti G, Sechi LA. Insulin receptors and renal sodium handling in hypertensive fructose-fed rats. Kidney Int 2003;64:2163–71. https://doi.org/10.1046/j.1523-1755.2003.00313.x.
[38] Tobar A, Ori Y, Benchetrit S, Milo G, Herman-Edelstein M, Zingerman B, et al. Proximal tubular hypertrophy and enlarged glomerular and proximal tubular urinary space in obese subjects with proteinuria. PLoS One 2013;8:e75547. https://doi.org/10.1371/journal.pone.0075547.
[39] Landau BR, Spring-Robinson CL, Muzic RFJ, Rachdaoui N, Rubin D, Berridge MS, et al. 6-Fluoro-6-deoxy-D-glucose as a tracer of glucose transport. Am J Physiol Endocrinol Metab 2007;293:E237–45. https://doi.org/10.1152/ajpendo.00022.2007.
[40] Ekberg K, Landau BR, Wajngot A, Chandramouli V, Efendic S, Brunengraber H, et al. Contributions by kidney and liver to glucose production in the postabsorptive state and after 60 h of fasting. Diabetes 1999;48:292–8. https://doi.org/10.2337/diabetes.48.2.292.
[41] Tripathy D, Solis-Herrera C, Chen X, Hansis-Diarte A, Chilton R, Defronzo RA, et al. Effect of dapagliflozin on renal and hepatic glucose kinetics in type 2 diabetes and NGT subjects. Diabetologia 2022.
[42] Nieth H, Schollmeyer P. Substrate-utilization of the human kidney. Nature 1966;209:1244–5. https://doi.org/10.1038/2091244a0.
[43] Wahren J, Felig P. Renal substrate exchange in human diabetes mellitus. Diabetes 1975;24:730–4. https://doi.org/10.2337/diab.24.8.730.
[44] Stumvoll M, Chintalapudi U, Perriello G, Welle S, Gutierrez O, Gerich J. Uptake and release of glucose by the human kidney. Postabsorptive rates and responses to epinephrine. J Clin Invest 1995;96:2528–33. https://doi.org/10.1172/JCI118314.
[45] Meyer C, Nadkarni V, Stumvoll M, Gerich J. Human kidney free fatty acid and glucose uptake: evidence for a renal glucose-fatty acid cycle. Am J Physiol 1997;273:E650–4. https://doi.org/10.1152/ajpendo.1997.273.3.E650.
[46] Meyer C, Stumvoll M, Nadkarni V, Dostou J, Mitrakou A, Gerich J. Abnormal renal and hepatic glucose metabolism in type 2 diabetes mellitus. J Clin Invest 1998;102:619–24. https://doi.org/10.1172/JCI2415.
[47] Meyer C, Woerle HJ, Dostou JM, Welle SL, Gerich JE. Abnormal renal, hepatic, and muscle glucose metabolism following glucose ingestion in type 2 diabetes. Am J Physiol Endocrinol Metab 2004;287:E1049–56. https://doi.org/10.1152/ajpendo.00041.2004.
[48] Baron AD, Steinberg H, Brechtel G, Johnson A. Skeletal muscle blood flow independently modulates insulin-mediated glucose uptake. Am J Physiol 1994;266:E248–53. https://doi.org/10.1152/ajpendo.1994.266.2.E248.
[49] Baron AD, Steinberg HO, Chaker H, Leaming R, Johnson A, Brechtel G. Insulin-mediated skeletal muscle vasodilation contributes to both insulin sensitivity and responsiveness in lean humans. J Clin Invest 1995;96:786–92. https://doi.org/10.1172/JCI118124.
[50] DeFronzo RA, Ferrannini E, Sato Y, Felig P, Wahren J. Synergistic interaction between exercise and insulin on peripheral glucose uptake. J Clin Invest 1981;68:1468–74. https://doi.org/10.1172/jci110399.